

Supplementary Materials to

Colorful Packages; Encapsulation of Fluorescent Proteins in Complex Coacervate Core Micelles

Antsje Nolles, Adrie H. Westphal, J. Mieke Kleijn, Willem J. H. van Berkel and Jan Willem Borst

Index

1. Sequence Identities and Multiple Structural Alignment of the Studied Fluorescent Proteins	2
2. Fluorescent Protein Characteristics.....	3
3. Dynamic Light Scattering Results	4
4. Fluorescence Correlation Spectroscopy Results.....	5
5. Absorption Spectral Analysis.....	6
6. Steady-State Fluorescence at Different pH Values.....	7
7. High Tension Graphs Related to the Far-UV CD Spectra.....	8
8. Sequence Alignment of All Fluorescent Proteins with Their Protein Data Bank Entries	9
9. References	13

1. Sequence Identities and Multiple Structural Alignment of the Studied Fluorescent Proteins

Table S1. Sequence identity percentages (%) between pairs of fluorescent proteins (FP variant) that have been studied.

FP variant	mEGFP	SBFP2	mTurquoise2	SYFP2	mKO2	TagRFP	mCherry
mEGFP	100	97.1	96.7	97.1	27.5	25.3	29.5
SBFP2	97.1	100	98.3	97.9	27.5	25.3	29.5
mTurquoise2	96.7	98.3	100	97.5	27.5	24.9	29.5
SYFP2	97.1	97.9	97.5	100	28.4	25.8	30.4
mKO2	27.5	27.5	27.5	28.4	100	47.1	48.5
TagRFP	25.3	25.3	24.9	25.8	47.1	100	56.9
mCherry	29.5	29.5	29.5	30.4	48.5	56.9	100

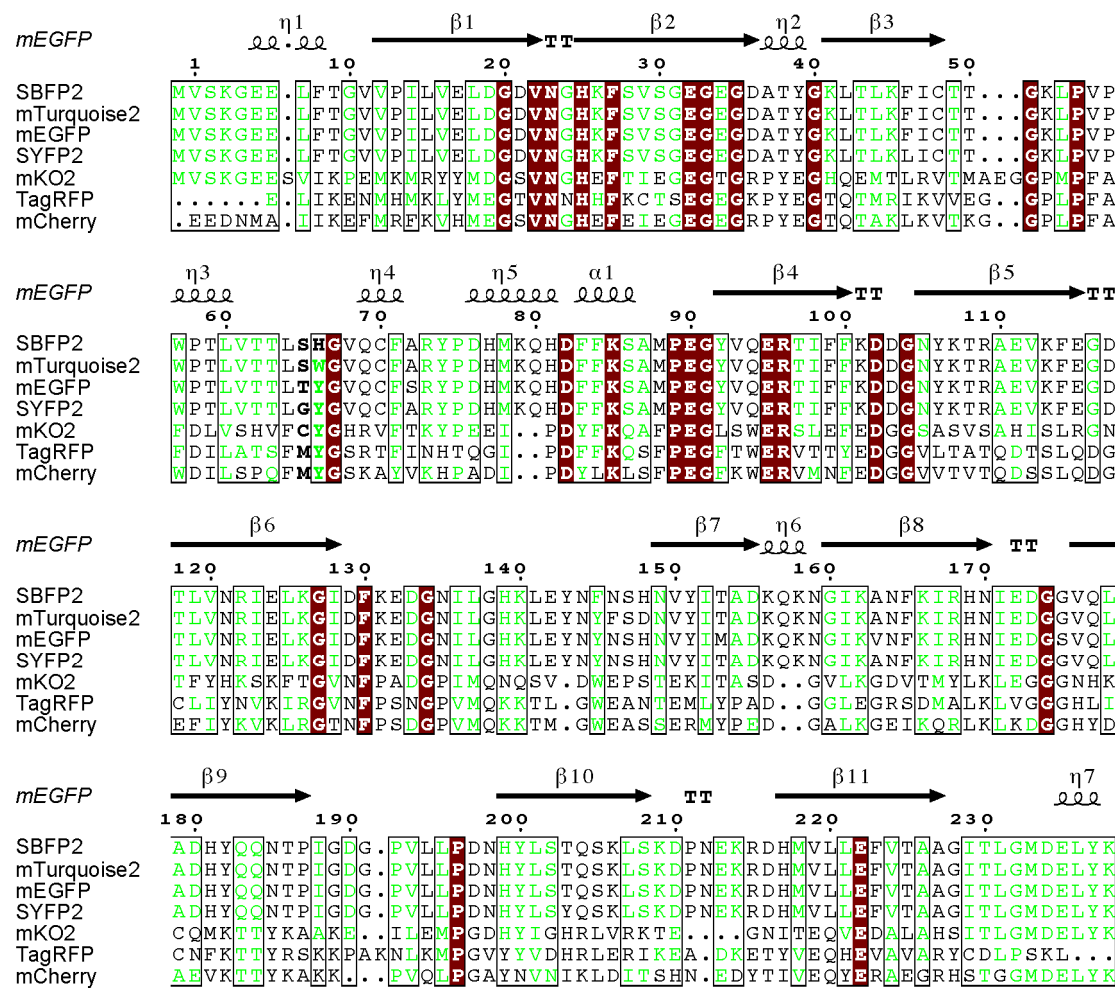


Figure S1. Multiple structural alignment of seven fluorescent proteins that were studied. Protein structures were aligned using msTALI software [1]. The alignment was then manually adjusted and drawn using ESPript 3.0 software [2]. Strictly conserved amino acid residues are shown with brown background and similar amino acid residues are boxed and shown in green. The amino acid residues forming the chromophore are indicated in bold letters. Secondary structure elements derived from mEGFP (PDB entry 4EUL [3]) are depicted as arrows (representing β -strands), coils (representing α - and 3^{10} -helices), and TT letters (representing turns). The numbering is based on that of mEGFP.

2. Fluorescent Protein Characteristics

Table S2 shows the characteristics of the studied fluorescent proteins (FPs). Next to the standard characteristics, some specific features for this article are given, *i.e.*, charge, monomeric quality and dissociation constant. The net charge of the FPs at pH 9.0 or pH 10.0 is given, which were calculated using the software package PROPKA 3.1 [4, 5]. The monomeric qualities of more than 40 FPs were determined by Cranfill, *et al.* [6]. For this, they fused FPs onto an endoplasmic reticulum (ER) membrane protein (CytERM). If the FP formed homo-oligomers due to high effective concentrations, the ER configured from a tubular network into an organized smooth ER whorl structure. The percentage of observed cells exhibiting an organized smooth ER whorl structure was related to the monomeric quality of the FPs. The dissociation constants were determined by sedimentation equilibrium analytical ultracentrifugation experiments. The A206K mutation introduced into yellow fluorescent protein (YFP) increased the dissociation constant from 0.11 to 74 mM [7]. This mutation is present in SBFP2, mTurquoise2, mEGFP, and SYFP2, providing these proteins with dissociation constants of about 74 mM. Next to that, mTurquoise2 bears the N146F mutation resulting in an increased dissociation constant [8]. The K_D of mKO2 is not determined so far. The dissociation constants of TagRFP and mCherry were investigated by Han, *et al.* [9]. For TagRFP a K_D of 0.038 mM was found and the K_D of mCherry was beyond the limit of their instrument.

Table S2. Properties of the studied fluorescent proteins (FP variant).

FP variant	λ_{ex} (nm)	λ_{em} (nm)	EC ($M^{-1} \text{ cm}^{-1}$)	QY	pKa	pI	Charge ^c	Monomeric quality (%) ^e	K_D (mM)	Reference
SBFP2	380	446	34000	0.47	5.5	5.59	-8.96	nd	74.0 ^{f,g}	Kremers, <i>et al.</i> [10]
mTurquoise2	434	474	30000	0.93	3.1	5.29	-11.30	93.8	> 74.0 ^{f,g,h}	Goedhart, <i>et al.</i> [11]
mEGFP	488	507	56000	0.60	6.0	5.49	-9.87	98.1	74.0 ^{f,g}	Yang, <i>et al.</i> [12]
SYFP2	515	527	101000	0.68	6.0	5.62	-9.75	nd	74.0 ^{f,g}	Kremers, <i>et al.</i> [13]
mKO2	551	565	63800	0.62	5.5	5.48	-13.09	68.4	nd	Sakaue-Sawano, <i>et al.</i> [14]
TagRFP	555	584	100000	0.48	3.8	7.43	-10.35 ^d	57.7	0.038 ⁱ	Merzlyak, <i>et al.</i> [15]
mCherry	587	610	72000	0.22	4.5 ^a , 10.3 ^b	5.70	-8.93	95.0	> 0.050 ⁱ	Shaner, <i>et al.</i> [16]

^afrom Shaner, *et al.* [16], ^bfrom Shu, *et al.* [17], ^cCharge based on PROPKA 3.1 results, determined at their respective pH value used for the experiments, ^dValue determined at pH 10, ^efrom Cranfill, *et al.* [6], ^ffrom Zacharias, *et al.* [7], ^gValue based on the presence of the A206K mutation, ^hfrom von Stetten, *et al.* [8], ⁱfrom Han, *et al.* [9], nd, not determined.

3. Dynamic Light Scattering Results

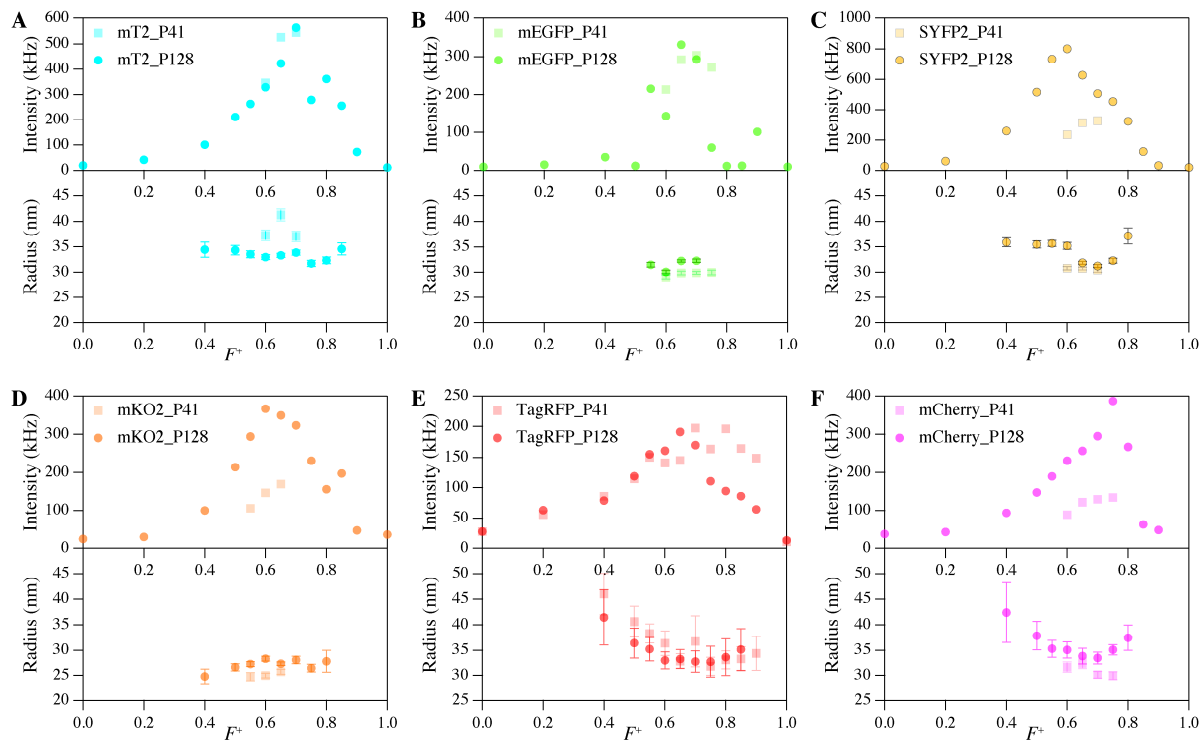


Figure S2. Dynamic light scattering composition results of (A) mTurquoise2 (mT2), (B) mEGFP, (C) SYFP2, (D) mKO2, (E) TagRFP, and (F) mCherry with P2MVP₄₁-*b*-PEO₂₀₅ (P41, light colored blocks) and P2MVP₁₂₈-*b*-PEO₄₇₇ (P128, dark colored circles) wherein the concentration of protein was kept constant. Top graphs show scattered intensity as a function of the F^+ composition, and bottom graphs show hydrodynamic radius as a function of the F^+ composition. Error bars show the distribution of radii in one experiment.

4. Fluorescence Correlation Spectroscopy Results

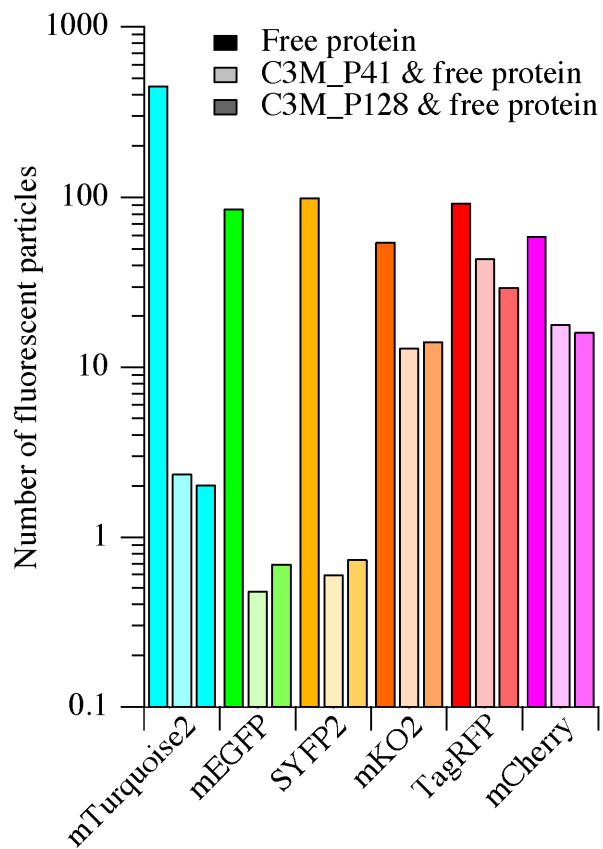


Figure S3. Fluorescence correlation spectroscopy results the number of fluorescent particles measured of all used FPs (except SBFP2) free in solution (darkest colored, left bars), and measured at the PMC with P2MVP₄₁-*b*-PEO₂₀₅ (C3M_P41, light colored, middle bars) and P2MVP₁₂₈-*b*-PEO₄₇₇ (C3M_P128, dark colored, right bars).

5. Absorption Spectral Analysis

Absorption spectra were recorded on a Hewlett Packard 8453 diode array spectrophotometer in 10 mM borate buffer at pH 9.0 for SBFP2, mTurquoise2, mEGFP, SYFP2, mKO2, and mCherry and at pH 10.0 for TagRFP at 20°C. Spectrophotometer settings were controlled using the UV-Visible ChemStation software package (Hewlett Packard, Palo Alto, CA, USA). Samples with concentrations of 1 μ M FP were measured free in buffered solution as well as encapsulated with P2MVP₄₁-*b*-PEO₂₀₅ and P2MVP₁₂₈-*b*-PEO₄₇₇ at their respective PMCs.

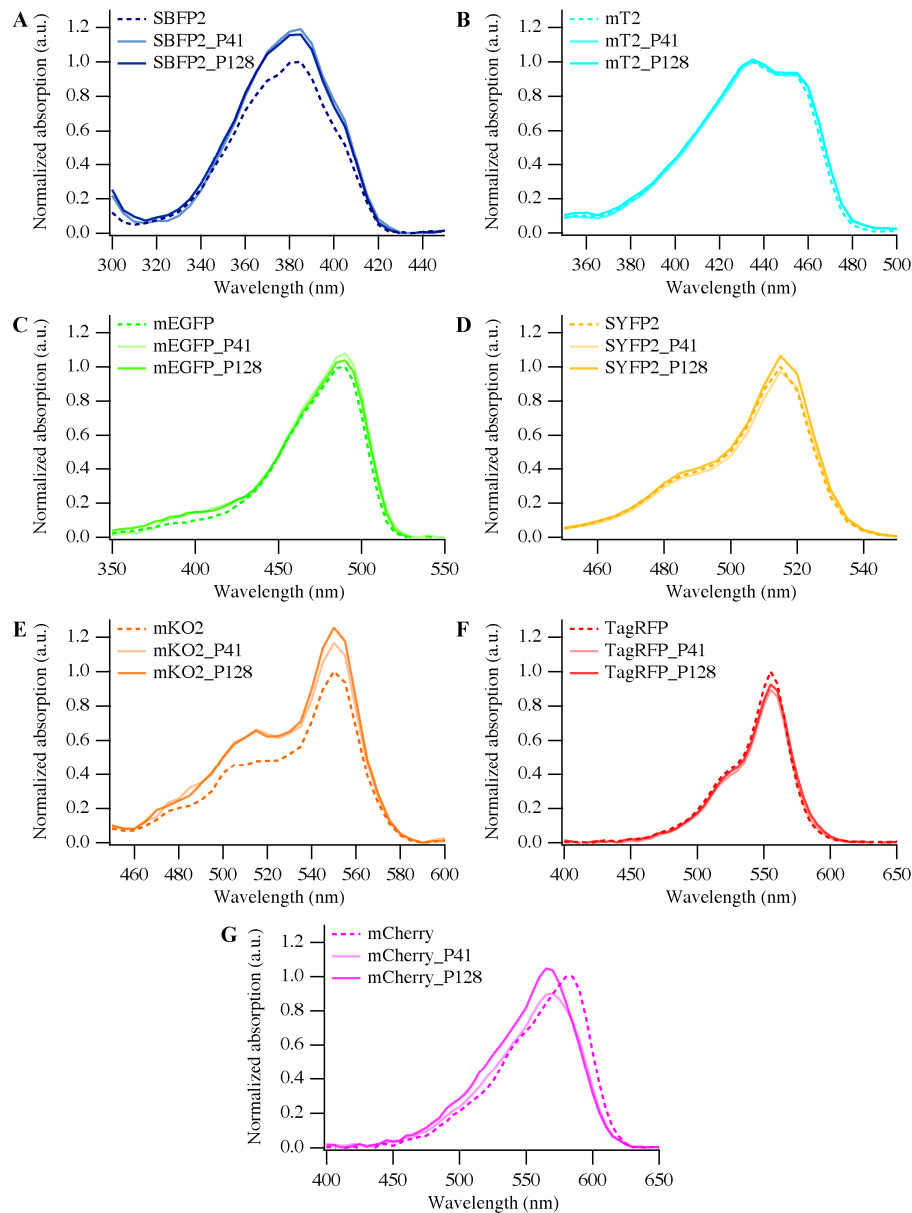


Figure S4. Normalized absorption spectra of (A) SBFP2, (B) mTurquoise2 (mT2), (C) mEGFP, (D) SYFP2, (E) mKO2, (F) TagRFP, and (G) mCherry for proteins free in solution (dashed lines) and encapsulated proteins in C3Ms at their respective PMCs with P2MVP₄₁-*b*-PEO₂₀₅ (P41, solid light colored line) and P2MVP₁₂₈-*b*-PEO₄₇₇ (P128, solid dark colored line). The spectra are normalized to those of the free proteins.

6. Steady-State Fluorescence at Different pH Values

Fluorescence excitation and emission spectra were measured using a Cary Eclipse spectrofluorimeter (Varian). Excitation and emission slits were set to yield bandwidths of 5 nm. All measurements were performed at 20°C. A master buffer was used consisting of 20 mM sodium phosphate, 20 mM citric acid, 10 mM glycine, and 150 mM NaCl adjusted to the desired pH by addition of NaOH. Samples with concentrations of 1 μ M FP at pH 5.2, 7.1, 9.0, and 10.0 were measured.

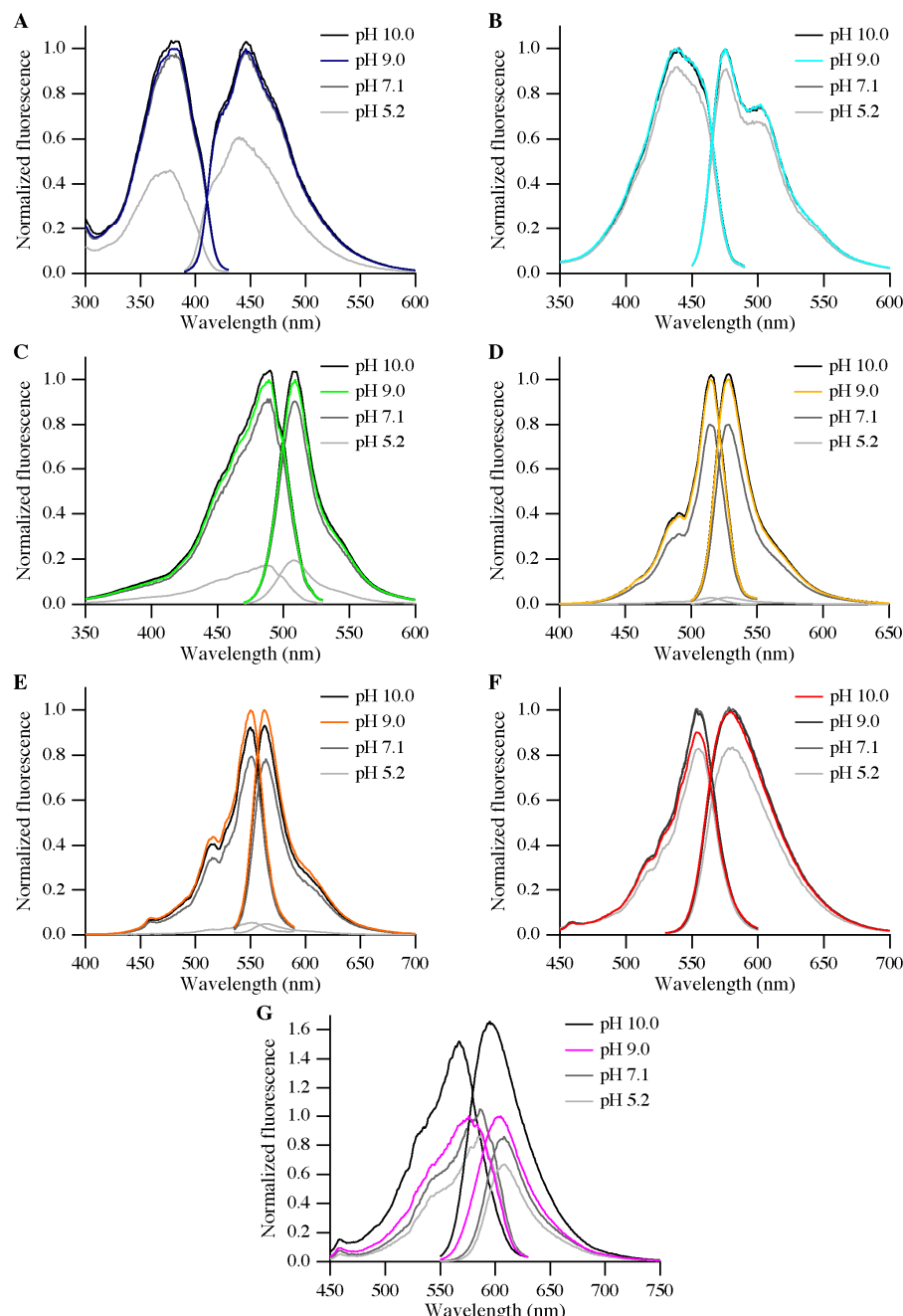


Figure S5. Normalized fluorescence excitation and emission spectra of (A) SBFP2, (B) mTurquoise2, (C) mEGFP, (D) SYFP2, (E) mKO2, (F) TagRFP, and (G) mCherry in solutions with different pH values. The spectra are colored according to the FP at the respective pH: pH 9.0 for SBFP2, mTurquoise2, mEGFP, SYFP2, mKO2, and mCherry and pH 10.0 for TagRFP. Spectra are normalized to the FPs at pH 9.0.

7. High Tension Graphs Related to the Far-UV CD Spectra

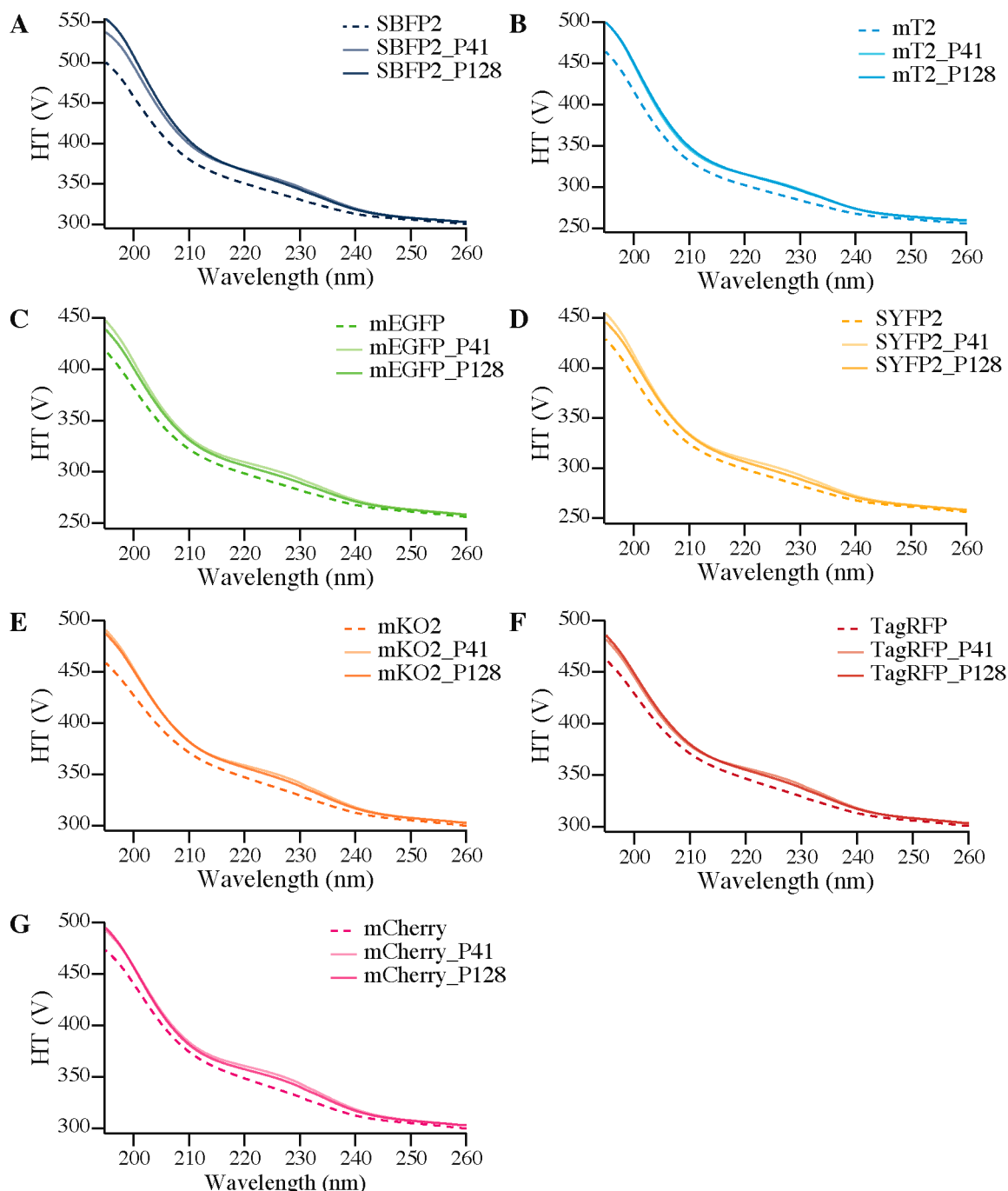


Figure S6. High tension (HT) signals of free fluorescent proteins (dashed lines) and encapsulated with P2MVP₄₁-*b*-PEO₂₀₅ (P41, solid light colored line) and P2MVP₁₂₈-*b*-PEO₄₇ (P128, solid dark colored line) belonging to the far-UV CD spectra in Figure 6: (A) SBFP2, (B) mTurquoise2 (mT2), (C) mEGFP, (D) SYFP2, (E) mKO2, (F) TagRFP, and (G) mCherry.

8. Sequence Alignment of All Fluorescent Proteins with Their Protein Data Bank Entries

	10	20	30	40	50	60
SBFP2	VSKGEELFTGVVPILVELGDPVNNGHKFSVS GE ^{GE} EGDATYGKLT L KFICTTGKLPVPWPTL					
	.:.					
1BFP	MSKGEELFTGVVPILVELGDPVNNGHKFSVS GE ^{GE} EGDATYGKLT L KFICTTGKLPVPWPTL					
	10	20	30	40	50	60
	70	80	90	100	110	120
SBFP2	VTTLSHGVCFCARYPDHM K QHDF F KSAMPEGYVQERTIFFKDDGNYKTRAEVKFEGDTLV					
	.:.:.:.:.:.:.:.:.:.:.:.:.:.:.:.:.					
1BFP	VTTFSHGVCFCRSY P DHMKRHDFFKSAMPEGYVQERTIFFKDDGNYKTRAEVKFEGDTLV					
	70	80	90	100	110	120
	130	140	150	160	170	180
SBFP2	NRIELKGIDFKEDGNILGHKLEYN N SHNVYITADKQKNGIKANFKIRHNIEDGGVQLAD					
	.:.:.:.:.:.:.:.:.:.:.:.:.:.					
1BFP	NRIELKGIDFKEDGNILGHKLEYN N SHNVYIMADKQKNGIKVNFKIRHNIEDGSVQLAD					
	130	140	150	160	170	180
	190	200	210	220	230	
SBFP2	HYQQNTPIGDGPVLLPDNHYLSTQSKLSKD P NEKRDHMVLLEFVTAAGITLGMDELYK					
	.:.:.:.:.:.:.:.					
1BFP	HYQQNTPIGDGPVLLPDNHYLSTQ S ALSKD P NEKRDHMVLLEFVTAAGITLGMDELYK					
	190	200	210	220	230	

Figure S7. Pairwise sequence alignment of SBFP2 with the template 1BFP generated by lalign [18]. The identical (double points) and similar (single point) residues are highlighted.

	10	20	30	40	50	60
mT2	MVS K GEELFTGVVPILVELGDPVNNGHKFSVS G E ^G EGDATYGKLT L KFICTTGKLPVPWPT					
	.:.:.:.:.:.:.:.:.					
3ZTF	MVS K GEELFTGVVPILVELGDPVNNGHKFSVS G E ^G EGDATYGKLT L KFICTTGKLPVPWPT					
	10	20	30	40	50	60
	70	80	90	100	110	120
mT2	LVTTLSHGVCFCARYPDHM K QHDF F KSAMPEGYVQERTIFFKDDGNYKTRAEVKFEGDTLV					
	.:.:.:.:.:.:.					
3ZTF	LVTTLSHGVCFCRSY P DHMKRHDFFKSAMPEGYVQERTIFFKDDGNYKTRAEVKFEGDTLV					
	70	80	90	100	110	120
	130	140	150	160	170	180
mT2	VNRIELKGIDFKEDGNILGHKLEYNYFSDNVYITADKQKNGIKANFKIRHNIEDGGVQLA					
	.:.:.:.:.:.					
3ZTF	VNRIELKGIDFKEDGNILGHKLEYNYFSDNVYITADKQKNGIKANFKIRHNIEDGGVQLA					
	130	140	150	160	170	180
	190	200	210	220	230	
mT2	DHYQQNTPIGDGPVLLPDNHYLSTQSKLSKD P NEKRDHMVLLEFVTAAGITLGMDELYK					
	.:.:.:.:.					
3ZTF	DHYQQNTPIGDGPVLLPDNHYLSTQ S ALSKD P NEKRDHMVLLEFVTAAGITLGMDELYK					
	190	200	210	220	230	

Figure S8. Pairwise sequence alignment of mTurquoise2 (mT2) with the template 3ZTF generated by lalign [18]. The identical (double points) and similar (single point) residues are highlighted.

	10	20	30	40	50	60
mEGFP	MVSKGEELFTGVVPILVELDGDVNNGHKFSVS	GEGE	GDATYGKLTLK	FIC	TGKLP	PWPWT

4EUL	MVSKGEELFTGVVPILVELDGDVNNGHKFSVS	GEGE	GDATYGKLTLK	FIC	TGKLP	PWPWT

	70	80	90	100	110	120
mEGFP	LVTTLTGYVQCFSRYPDHM	QHDF	FFKSAMPEGYVQERTIFFKDDGNYK	TRAEVK	FEGDTL	

4EUL	LVTTLTGYVQCFSRYPDHM	QHDF	FFKSAMPEGYVQERTIFFKDDGNYK	TRAEVK	FEGDTL	

	130	140	150	160	170	180
mEGFP	VNRIELKGIDFKEDGNILGHKLEYNN	YNSHN	VIMADKQKNGIKVN	FIRHNIEDGSV	QLA	

4EUL	VNRIELKGIDFKEDGNILGHKLEYNN	YNSHN	VIMADKQKNGIKVN	FIRHNIEDGSV	QLA	

	190	200	210	220	230	
mEGFP	DHYQQNTPIGDGPVLLPDNHYLSTQSKL	S	KDPNEKR	DHMVL	LEFVT	AAGITLGMD
	LYK
4EUL	DHYQQNTPIGDGPVLLPDNHYLSTQSKL	S	KDPNEKR	DHMVL	LEFVT	AAGITLGMD
	LYK
	190	200	210	220	230	

Figure S9. Pairwise sequence alignment of mEGFP with the template 4EUL generated by lalign [18]. The identical (double points) and similar (single point) residues are highlighted.

	10	20	30	40	50	60
SYFP2	MVSKGEELFTGVVPILVELDGDVNNGHKFSVS	GEGE	GDATYGKLTLK	LIC	TGKLP	PWPWT

1MYW	MVSKGEELFTGVVPILVELDGDVNNGHKFSVS	GEGE	GDATYGKLTLK	LIC	TGKLP	PWPWT

	70	80	90	100	110	120
SYFP2	LVTTLGYVQCFARYPDHM	QHDF	FFKSAMPEGYVQERTIFFKDDGNYK	TRAEVK	FEGDTL	

1MYW	LVTTLGYGLQCFARYPDHM	QHDF	FFKSAMPEGYVQERTIFFKDDGNYK	TRAEVK	FEGDTL	

	130	140	150	160	170	180
SYFP2	VNRIELKGIDFKEDGNILGHKLEYNN	YNSHN	VITADKQKNGIKANF	KIRHNIEDGGV	QLA	

1MYW	VNRIELKGIDFKEDGNILGHKLEYNN	YNSHN	VITADKQKNGIKANF	KIRHNIEDGGV	QLA	

	190	200	210	220	230	
SYFP2	DHYQQNTPIGDGPVLLPDNHYL	S	YQSKL	S	KDPNEKR	DHMVL
	LEFVT
1MYW	DHYQQNTPIGDGPVLLPDNHYL	S	YQSKL	S	KDPNEKR	DHMVL
	LEFVT
	190	200	210	220	230	

Figure S10. Pairwise sequence alignment of SYFP2 with the template 1MYW generated by lalign [18]. The identical (double points) and similar (single point) residues are highlighted.

	10	20	30	40	50	60
mKO2	SVIKPEMKMRYYMDGSVNGHEFTIEGEGTGRPYEGHQEMTLRVTMAEGGPMPFAFDILVSH					
	:::::::	:::::::	:::::::	:::::::	:::::::	:::::::
2ZMU	SVIKPEMKMRYYMDGSVNGHEFTIEGEGTGRPYEGHQEMTLRVTMAKGPMPPFAFDILVSH					
	10	20	30	40	50	60
	70	80	90	100	110	120
mKO2	VFCYGHGVFTKYPEEIPDYFKQAFPEGLSWERSLEFEDGGSASVSAHISLRGNTFYHKSK					
	:::::	:::::	:::::	:::::	:::::	:::::
2ZMU	VFCYGHRPFTKYPEEIPDYFKQAFPEGLSWERSLEFEDGGSASVSAHISLRGNTFYHKSK					
	70	80	90	100	110	120
	130	140	150	160	170	180
mKO2	FTGVNFPADGPIMQNQSVDWEPSTEKITASDGVLKGVDVTMYLKLEGGGNHKCQMKTTYKA					
	:::::	:::::	:::::	:::::	:::::	:::::
2ZMU	FTGVNFPADGPIMQNQSVDWEPSTEKITASDGVLKGVDVTMYLKLEGGGNHKCQFKTTYKA					
	130	140	150	160	170	180
	190	200	210	220		
mKO2	AKEILEMPGDHYIGHRLVRKTEGNITEQVEDALAHs					
	:::::	:::::	:::::	:::::	:::::	:::::
2ZMU	AKKILKMPGSHYISHRLVRKTEGNITELVEDAVAHS					
	190	200	210			

Figure S11. Pairwise sequence alignment of mKO2 with the template 2ZMU generated by lalign [18]. The identical (double points) and similar (single point) residues are highlighted.

	10	20	30	40	50	60
TagRFP	MVSKGEELIKENMHMKLYMEGTVNHHFKCTSEGECKPYEGTQTMRIKVVEGGPLPFAFD					
	:::::::	:::::::	:::::::	:::::::	:::::::	:::::::
3M22	MVSKGEELIKENMHMKLYMEGTVNHHFKCTSEGECKPYEGTQTMRIKVVEGGPLPFAFD					
	10	20	30	40	50	60
	70	80	90	100	110	120
TagRFP	ILATSFMYGSRTFINHTQGIPDFFKQSFPEGFTWERVTTYEDGGVLTATQDTSLQDGCLI					
	:::::	:::::	:::::	:::::	:::::	:::::
3M22	ILATSFMYGSRTFINHTQGIPDFFKQSFPEGFTWERVTTYEDGGVLTATQDTSLQDGCLI					
	70	80	90	100	110	120
	130	140	150	160	170	180
TagRFP	YNVKIRGVNFPNSGPVMQKKTLGWEANTEMLYPADGGLEGRSDMALKLVGGGLICNFKT					
	:::::	:::::	:::::	:::::	:::::	:::::
3M22	YNVKIRGVNFPNSGPVMQKKTLGWEANTEMLYPADGGLEGRSDMALKLVGGGLICNFKT					
	130	140	150	160	170	180
	190	200	210	220	230	
TagRFP	TYRSKKPAKNLKMGPVYYVDHRLERIKEADKETYVEQHEAVARYCDLPSKLLYK					
	:::::	:::::	:::::	:::::	:::::	..
3M22	TYRSKKPAKNLKMGPVYYVDHRLERIKEADKETYVEQHEAVARYCDLPSKLGHK					
	190	200	210	220	230	

Figure S12. Pairwise sequence alignment of TagRFP with the template 3M22 generated by lalign [18]. The identical (double points) and similar (single point) residues are highlighted.

	10	20	30	40	50	60
mCherry	MVSKGEEDNMAIIKEFMRFKVHMEGSVNGHEFEIEGEGEGRPYEGTQTAKLKVTKGGPLP	:::::::::::::::::::	:::::::::::::::::::	:::::::::::::::::::	:::::::::::::::::::	:::::::::::::::::::
2H5Q	MVSKGEEDNMAIIKEFMRFKVHMEGSVNGHEFEIEGEGEGRPYEGTQTAKLKVTKGGPLP	10	20	30	40	50
						60
	70	80	90	100	110	120
mCherry	FAWDILSPQFMYGSKAYVKHPADIPDYLKLSFPEGFKWERVMNFEDGGVVTVTQDSSLQD	:::::::::::::::::::	:::::::::::::::::::	:::::::::::::::::::	:::::::::::::::::::	:::::::::::::::::::
2H5Q	FAWDILSPQFMYGSKAYVKHPADIPDYLKLSFPEGFKWERVMNFEDGGVVTVTQDSSLQD	70	80	90	100	110
						120
	130	140	150	160	170	180
mCherry	GEFIYKVKLRLGTNFPSDGPVMQKKTMGWEASSERMYPEDGALKGEIKQLKLKDGGHYDA	:::::::::::::::::::	:::::::::::::::::::	:::::::::::::::::::	:::::::::::::::::::	:::::::::::::::::::
2H5Q	GEFIYKVKLRLGTNFPSDGPVMQKKTMGWEASSERMYPEDGALKGEIKQLKLKDGGHYDA	130	140	150	160	170
						180
	190	200	210	220	230	
mCherry	EVKTTYKAKKPVQLPGAYNVNIKLDITSHNEDYTIVEQYERAEGRHSTGGMDELYK	:::::::::::::::::::	:::::::::::::::::::	:::::::::::::::::::	:::::::::::::::::::	
2H5Q	EVKTTYKAKKPVQLPGAYNVNIKLDITSHNEDYTIVEQYERAEGRHSTGGMDELYK	190	200	210	220	230

Figure S13. Pairwise sequence alignment of mCherry with the template 2H5Q generated by lalign [18]. The identical (double points) and similar (single point) residues are highlighted.

9. References

1. Shealy, P.; Valafar, H., Multiple structure alignment with msTALI. *BMC Bioinf.* **2012**, *13*, 105.
2. Robert, X.; Gouet, P., Deciphering key features in protein structures with the new ENDscript server. *Nucleic Acids Res.* **2014**, *42*, (Web Server issue), W320-324.
3. Arpino, J. A.; Rizkallah, P. J.; Jones, D. D., Crystal structure of enhanced green fluorescent protein to 1.35 Å resolution reveals alternative conformations for Glu222. *PLoS ONE* **2012**, *7*, e47132.
4. Rostkowski, M.; Olsson, M. H. M.; Søndergaard, C. R.; Jensen, J. H., Graphical analysis of pH-dependent properties of proteins predicted using PROPKA. *BMC Struct. Biol.* **2011**, *11*, 6.
5. Olsson, M. H.; Søndergaard, C. R.; Rostkowski, M.; Jensen, J. H., PROPKA3: Consistent treatment of internal and surface residues in empirical pKa predictions. *J. Chem. Theory Comput.* **2011**, *7*, 525-537.
6. Cranfill, P. J.; Sell, B. R.; Baird, M. A.; Allen, J. R.; Lavagnino, Z.; de Gruiter, H. M.; Kremers, G. J.; Davidson, M. W.; Ustione, A.; Piston, D. W., Quantitative assessment of fluorescent proteins. *Nat. Methods* **2016**, *13*, 557-562.
7. Zacharias, D. A.; Violin, J. D.; Newton, A. C.; Tsien, R. Y., Partitioning of lipid-modified monomeric GFPs into membrane microdomains of live cells. *Science* **2002**, *296*, 913-916.
8. von Stetten, D.; Noirclerc-Savoye, M.; Goedhart, J.; Gadella, T. W., Jr.; Royant, A., Structure of a fluorescent protein from *Aequorea victoria* bearing the obligate-monomer mutation A206K. *Acta Crystallogr., Sect. F: Struct. Biol. Cryst. Commun.* **2012**, *68*, 878-882.
9. Han, L.; Zhao, Y.; Zhang, X.; Peng, J.; Xu, P.; Huan, S.; Zhang, M., RFP tags for labeling secretory pathway proteins. *Biochem. Biophys. Res. Commun.* **2014**, *447*, 508-512.
10. Kremers, G. J.; Goedhart, J.; van den Heuvel, D. J.; Gerritsen, H. C.; Gadella, T. W. J., Improved green and blue fluorescent proteins for expression in bacteria and mammalian cells. *Biochemistry* **2007**, *46*, 3775-3783.
11. Goedhart, J.; von Stetten, D.; Noirclerc-Savoye, M.; Lelimousin, M.; Joosen, L.; Hink, M. A.; van Weeren, L.; Gadella, T. W. J.; Royant, A., Structure-guided evolution of cyan fluorescent proteins towards a quantum yield of 93%. *Nat. Commun.* **2012**, *3*, 751.
12. Yang, T. T.; Cheng, L.; Kain, S. R., Optimized codon usage and chromophore mutations provide enhanced sensitivity with the green fluorescent protein. *Nucleic Acids Res.* **1996**, *24*, 4592-4593.
13. Kremers, G. J.; Goedhart, J.; van Munster, E. B.; Gadella, T. W. J., Cyan and yellow super fluorescent proteins with improved brightness, protein folding, and FRET Forster radius. *Biochemistry* **2006**, *45*, 6570-6580.
14. Sakaue-Sawano, A.; Kurokawa, H.; Morimura, T.; Hanyu, A.; Hama, H.; Osawa, H.; Kashiwagi, S.; Fukami, K.; Miyata, T.; Miyoshi, H.; Imamura, T.; Ogawa, M.; Masai, H.; Miyawaki, A., Visualizing spatiotemporal dynamics of multicellular cell-cycle progression. *Cell* **2008**, *132*, 487-498.
15. Merzlyak, E. M.; Goedhart, J.; Shcherbo, D.; Bulina, M. E.; Shcheglov, A. S.; Fradkov, A. F.; Gaintzeva, A.; Lukyanov, K. A.; Lukyanov, S.; Gadella, T. W. J.; Chudakov, D. M., Bright monomeric red fluorescent protein with an extended fluorescence lifetime. *Nat. Methods* **2007**, *4*, 555-557.
16. Shaner, N. C.; Campbell, R. E.; Steinbach, P. A.; Giepmans, B. N.; Palmer, A. E.; Tsien, R. Y., Improved monomeric red, orange and yellow fluorescent proteins derived from *Discosoma sp.* red fluorescent protein. *Nat. Biotechnol.* **2004**, *22*, 1567-1572.
17. Shu, X.; Shaner, N. C.; Yarbrough, C. A.; Tsien, R. Y.; Remington, S. J., Novel chromophores and buried charges control color in mFruits. *Biochemistry* **2006**, *45*, 9639-9647.
18. Huang, X. Q.; Miller, W., A time-efficient, linear-space local similarity algorithm. *Adv. Appl. Math.* **1991**, *12*, 337-357.